Rovibrational Quantum Dynamics of the Methane-Water Dimer

János Sarka,[1,2] Attila Császár,[1,2] Edit Mátyus[1]

[1]Laboratory of Molecular Structure and Dynamics
Eötvös Loránd University
Budapest, Hungary

[2]MTA-ELTE Complex Chemical Systems Research Group
Budapest, Hungary

Outline of the talk

- Introduction
- Variational rovibrational computations
- Rovibrational results for $CH_4 \cdot H_2O$: theory vs. experiment
- Deuterated isotopologues
- The coupled-rotors picture

Outline of the talk

- Introduction
- Variational rovibrational computations
- Rovibrational results for $CH_4 \cdot H_2O$: theory vs. experiment
- Deuterated isotopologues
- The coupled-rotors picture

Experimental results

High-resolution far-infrared spectroscopic measurements

"In all, 950 peaks have been recorded, and we have been able to give an unambiguous rotational assignment for 329 of them, as described in the following sections."

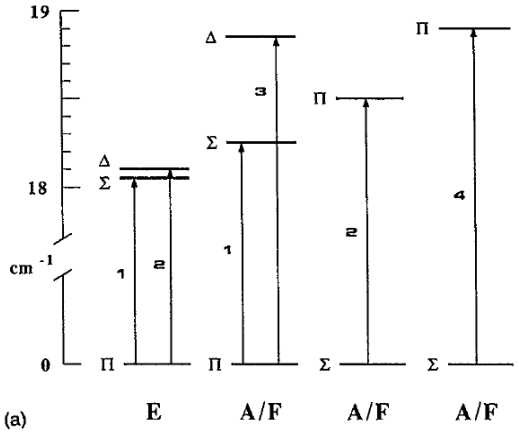

ortho

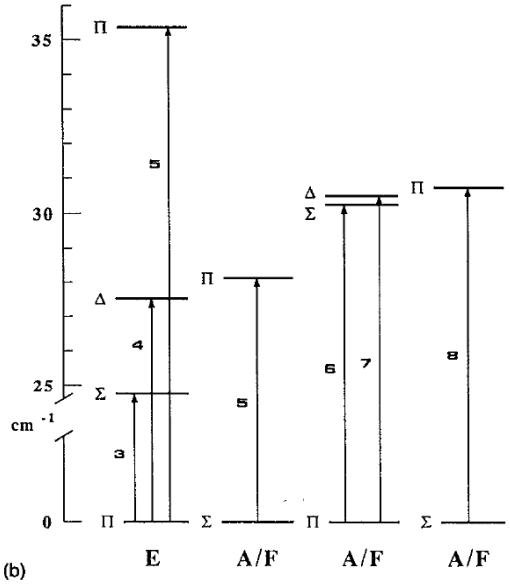

para

L. Dore, R. C. Cohen, C. A. Schmuttenmaer, K. L. Busarow, M. J. Elrod, J. G. Loeser, and R. J. Saykally, J. Chem. Phys. 100, 863 (1994).

Microwave spectrum

R. D. Suenram and G. T. Fraser and F. J. Lovas and Y. Kawashima, J. Chem. Phys. 101, 7230 (1994).

Electronic structure computations

- intermolecular (6D) PES: O. Akin-Ojo and K. Szalewicz, J. Chem. Phys. 123, 134311 (2005).
- full (18D) PES: C. Qu, R. Conte, P. L. Houston, and J. M. Bowman, PCCP 17, 8172 (2015).

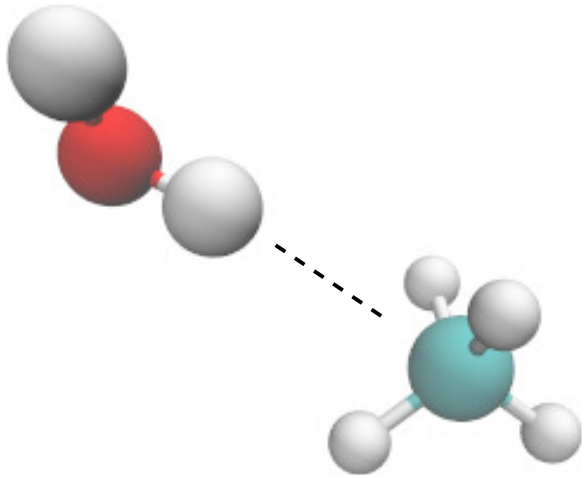

Global minimum (GM) (0 cm^{-1})
H_2O is the proton donor

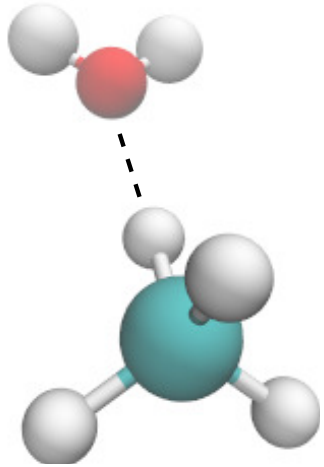

Secondary minimum (SM) (99 cm^{-1})
CH_4 is the proton donor

- equilibrium structures: C_s point group symmetry
- intermolecular dissociation energy from the GM: $D_e \approx 350$ cm^{-1}, $D_0 \approx 150$ cm^{-1}

Molecular symmetry group: G_{48}

$2! \cdot 4! \cdot 2/2 = 48$ permutation inversion versions with feasible exchange

E, (ab)

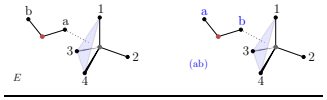

$\{(123)\}_{n_{\mathrm{cl}}=8}$, $\{(123)(\mathrm{ab})\}_{n_{\mathrm{cl}}=8}$

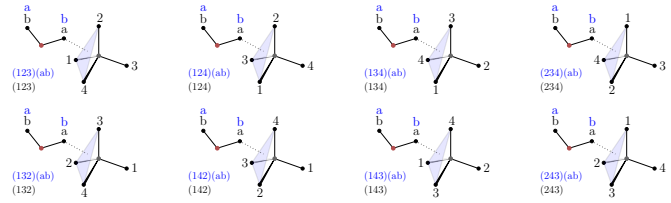

$\{(12)(34)\}_{n_{\mathrm{cl}}=3}$, $\{(12)(34)(\mathrm{ab})\}_{n_{\mathrm{cl}}=3}$

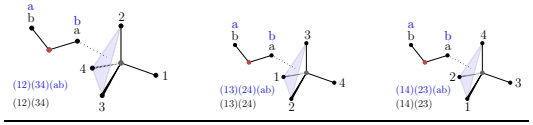

$\{[(1234)]^*\}_{n_{\mathrm{cl}}=6}$, $\{[(1234)(\mathrm{ab})]^*\}_{n_{\mathrm{cl}}=6}$

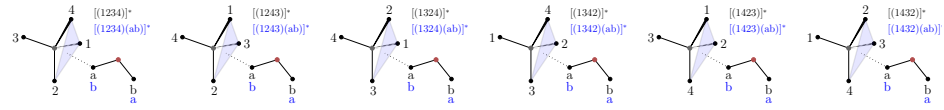

$\{[(23)]^*\}_{n_{\mathrm{cl}}=6}$, $\{[(23)(\mathrm{ab})]^*\}_{n_{\mathrm{cl}}=6}$

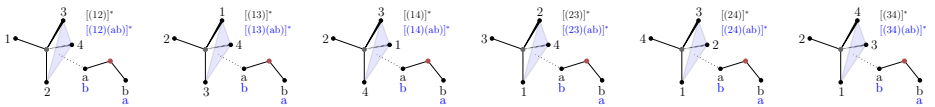

Molecular symmetry group: G_{48}

G_{48}	E	(123)	(14)(23)	[(1423)(ab)]*	[(23)(ab)]*	(ab)	(123)(ab)	(14)(23)(ab)	[(1423)]*	[(23)]*
n_{cl}	1	8	3	6	6	1	8	3	6	6
A_1^+	1	1	1	1	1	1	1	1	1	1
A_2^+	1	1	1	−1	−1	1	1	1	−1	−1
E^+	2	−1	2	0	0	2	−1	2	0	0
F_1^+	3	0	−1	1	−1	3	0	−1	1	−1
F_2^+	3	0	−1	−1	1	3	0	−1	−1	1
A_1^-	1	1	1	1	1	−1	−1	−1	−1	−1
A_2^-	1	1	1	−1	−1	−1	−1	−1	1	1
E^-	2	−1	2	0	0	−2	1	−2	0	0
F_1^-	3	0	−1	1	−1	−3	0	1	−1	1
F_2^-	3	0	−1	−1	1	−3	0	1	1	−1

no proton exchange between the moieties:
CH_4·(ortho-H_2O) (Γ^-) and CH_4·(para-H_2O) (Γ^+)

alternatively: CH_4·(ortho-H_2O) (Γ_a) and CH_4·(para-H_2O) (Γ_s)

Tunneling splitting

- 48 equivalent minima
- 24 functions of A' and A" symmetries of the C_s group (symmetry of the equilibrium structure):

$$\Gamma_{A'} = A_1^+ \oplus E^+ \oplus F_1^+ \oplus 2F_2^+ \oplus A_2^- \oplus E^- \oplus 2F_1^- \oplus F_2^-$$

$\Rightarrow$ symmetry of the $J = 0$ ZPV splitting manifold

$$\Gamma_{A''} = A_2^+ \oplus E^+ \oplus 2F_1^+ \oplus F_2^+ \oplus A_1^- \oplus E^- \oplus F_1^- \oplus 2F_2^-$$

J. Sarka, A. G. Császár, S. C. Althorpe, D. J. Wales, and E. Mátyus, Phys. Chem. Chem. Phys. 18, 22816 (2016).

Outline of the talk

- Introduction
- Variational rovibrational computations
- Rovibrational results for $CH_4 \cdot H_2O$: theory vs. experiment
- Deuterated isotopologues
- The coupled-rotors picture

GENIUSH approach

General (GE) rovibrational code with numerical (N), internal-coordinate (I), user-specified (US) Hamiltonian (H).

Rovibrational Hamiltonian in the Podolsky form

$$\hat{H}^{\mathrm{P}} = \frac{1}{2} \sum_{k=1}^{D+3} \sum_{l=1}^{D+3} \tilde{g}^{-1/4} \hat{p}_k G_{kl} \tilde{g}^{1/2} \hat{p}_l \tilde{g}^{-1/4} + V \qquad (1)$$

Mass-weighted metric tensor ($k, l = 1, 2, \ldots, D+3$):

$$g_{kl} = \sum_{i=1}^{N} m_i \left(\frac{\partial \boldsymbol{r}_i}{\partial q_k} \right)^{\mathrm{T}} \left(\frac{\partial \boldsymbol{r}_i}{\partial q_l} \right) \qquad (2)$$

$$\boldsymbol{G} = \boldsymbol{g}^{-1} \quad \text{and} \quad \tilde{g} = \det \boldsymbol{g} \qquad (3)$$

Angular momentum operators ($a = 1, 2, 3$):

$$\hat{p}_{D+a} = -\mathrm{i}\hbar \frac{\partial}{\partial q_{D+a}} = \hat{J}_a \qquad (4)$$

- $D \leq 3N - 6$: **reduced and full-dimensional models**

(Quasi-)variational solution

- vibrational representation: Hermite, Legendre, Laguerre, Fourier, potential-optimized, etc. DVRs
- rotational representation: Wang functions
- PES: $\boldsymbol{V}(\boldsymbol{q})$: diagonal matrix
- KEO: $\boldsymbol{g}(\boldsymbol{q})$, $\tilde{g}(\boldsymbol{q})$, $\boldsymbol{G}(\boldsymbol{q})$: diagonal matrices
- Lanczos iterative eigensolver

Advantages of GENIUSH

- arbitrary internal coordinates
- arbitrary embeddings
- no in principle limit on the size of the molecule

E. Mátyus, G. Czakó, and A. G. Császár, J. Chem. Phys. 130, 134112 (2009);
C. Fábri, E. Mátyus, and A. G. Császár, J. Chem. Phys. 134, 074105 (2011).

Rovibrational computational details

Internal coordinates

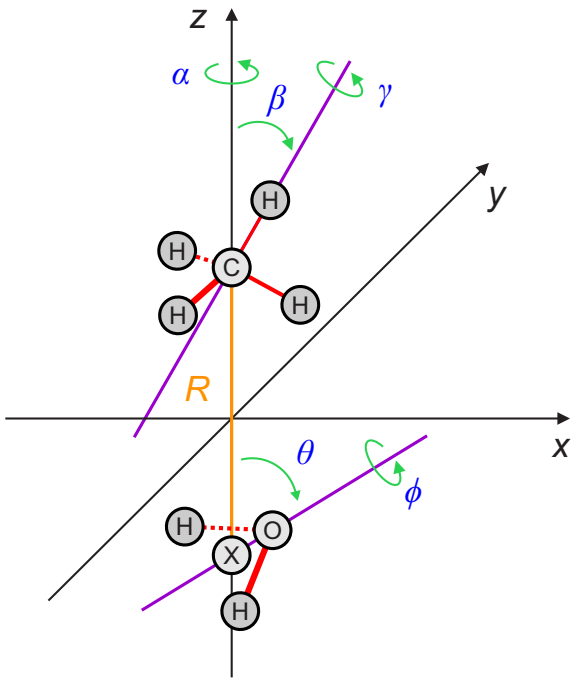

relative motion of rigid monomers

Discrete variable representations

Coord.	Min.[a]	Nuclear motion computations		
		DVR type[b]	N	Grid interval
R [Å]	3.447	PO Laguerre	15	scaled to [2.5,6.0]
θ [°]	117.72	PO Legendre	14	scaled to [1,179]
ϕ [°]	90.00	Exponential	15	unscaled on [0,360)
α [°]	297.65	Exponential	9	unscaled on [0,360)
β [°]	112.80	PO Legendre	21	scaled to [1,179]
γ [°]	293.52	Exponential	21	unscaled on [0,360)

J. Sarka, A. G. Császár, S. C. Althorpe, D. J. Wales, and E. Mátyus, PCCP 18, 22816 (2016).
J. Sarka, A. G. Császár, and E. Mátyus, PCCP 19, 15335 (2017).

Outline of the talk

- Introduction
- Variational rovibrational computations
- Rovibrational results for $CH_4 \cdot H_2O$: theory vs. experiment
- Deuterated isotopologues
- The coupled-rotors picture

$CH_4 \cdot H_2O$: vibrational states

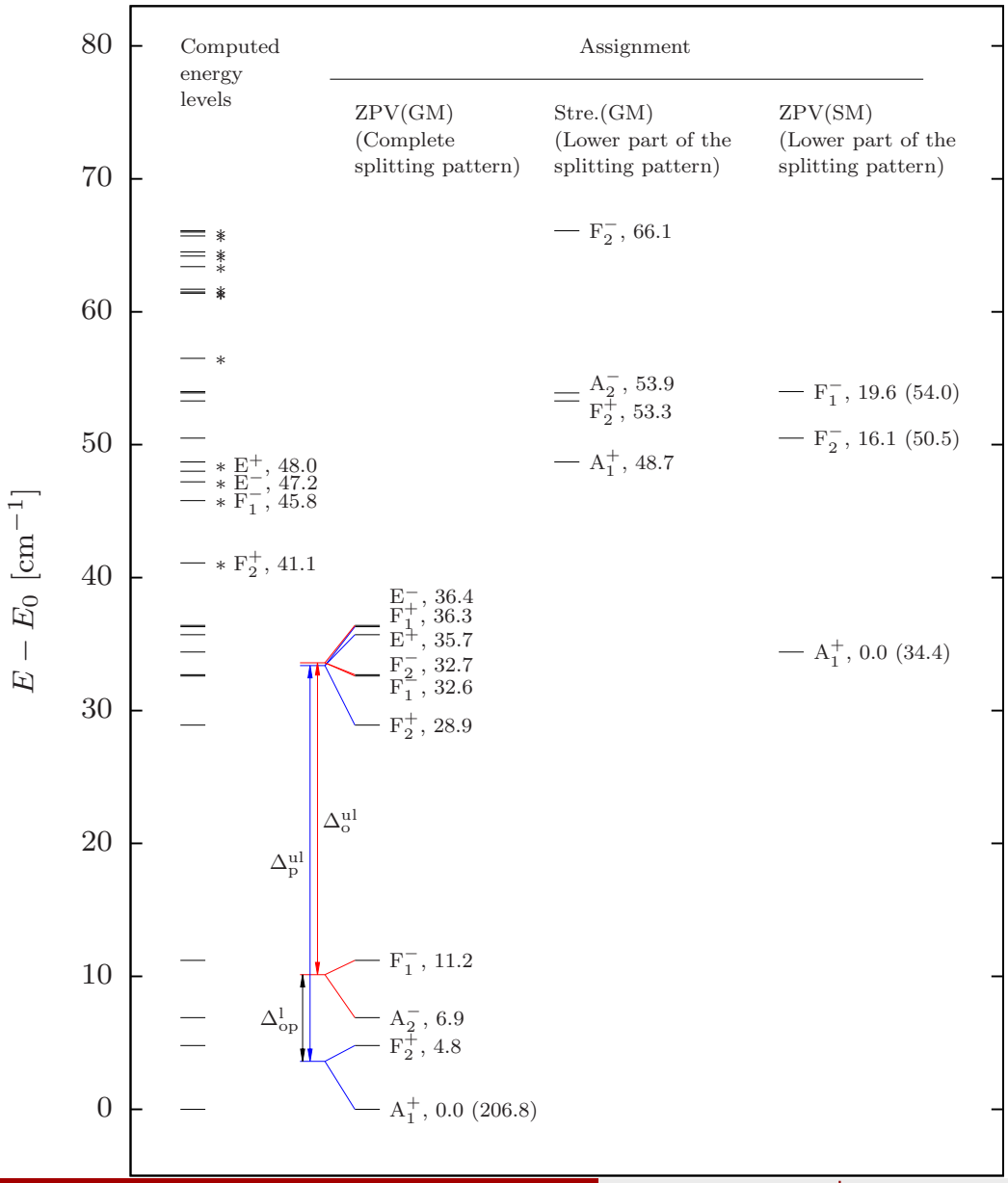

Assignment (example)

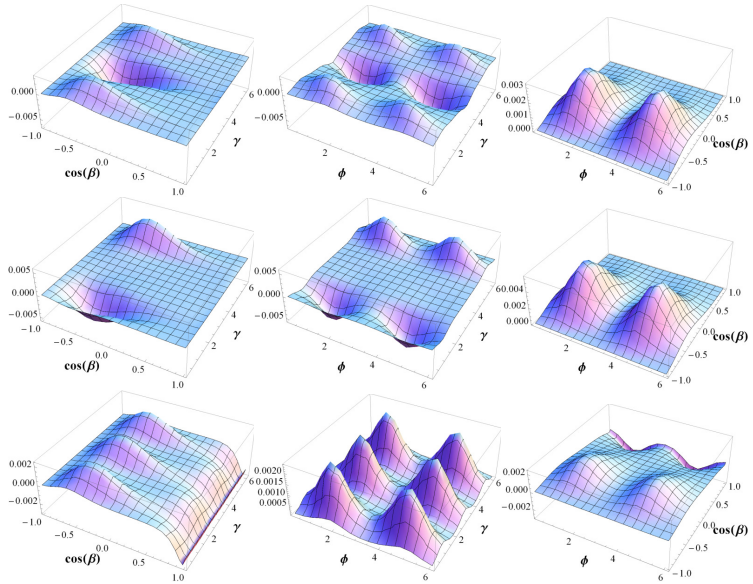

$CH_4 \cdot$(para-H_2O): F_2^+ (4.8 cm^{-1})

J. Sarka, A. G. Császár, S. C. Althorpe, D. J. Wales, and E. Mátyus, Phys. Chem. Chem. Phys. 18, 22816 (2016).

CH_4·(ortho-H_2O): transitions seen in the experiment

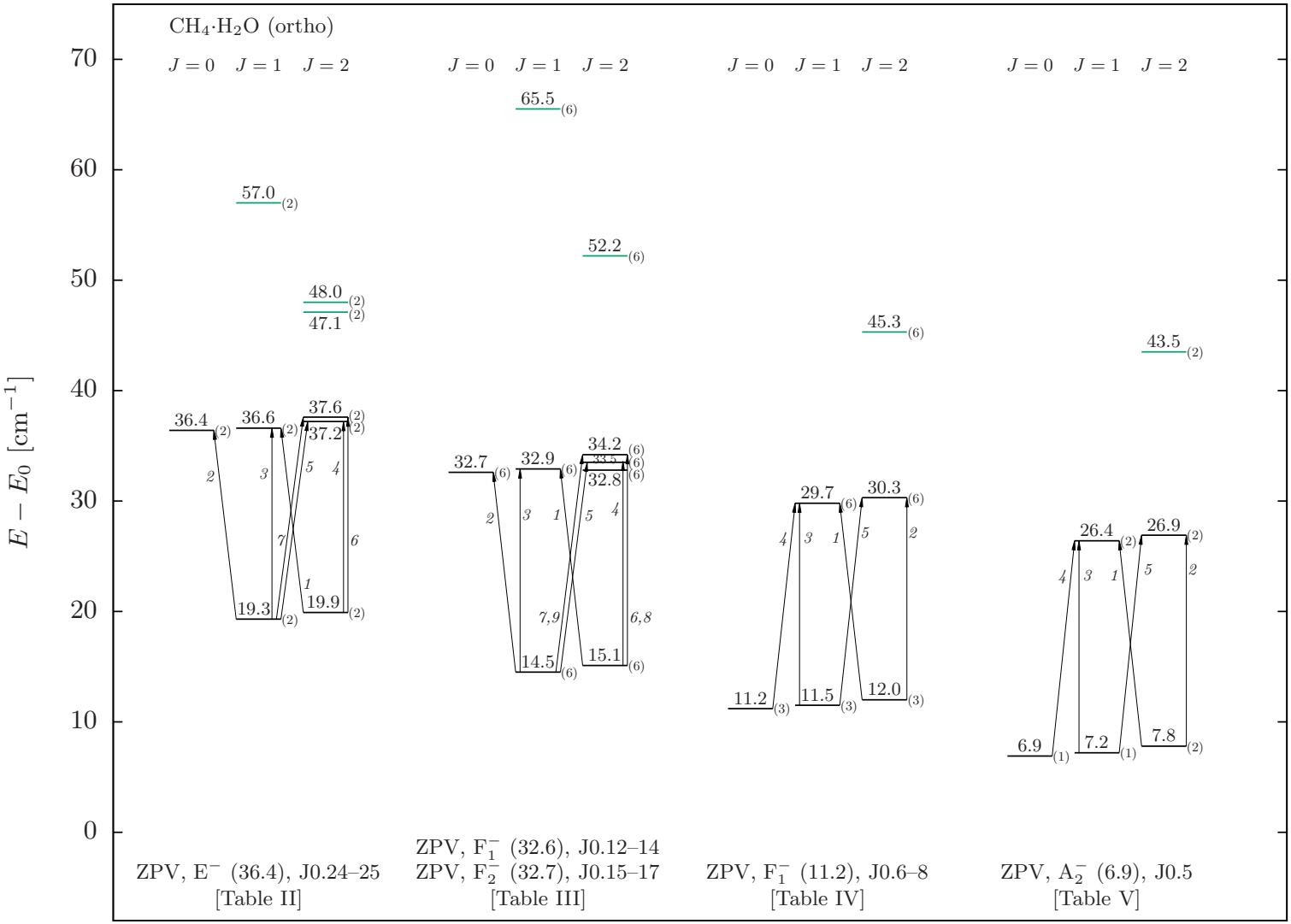

Deviation from experiment:
$(\Delta, \sigma) = (0.5, 0.005)$ cm^{-1}

[Exp.: JCP 100, 863 (1994)]

J. Sarka, A. G. Császár, S. C. Althorpe, D. J. Wales, and E. Mátyus, Phys. Chem. Chem. Phys. 18, 22816 (2016).

CH_4·(para-H_2O): transitions seen in the experiment

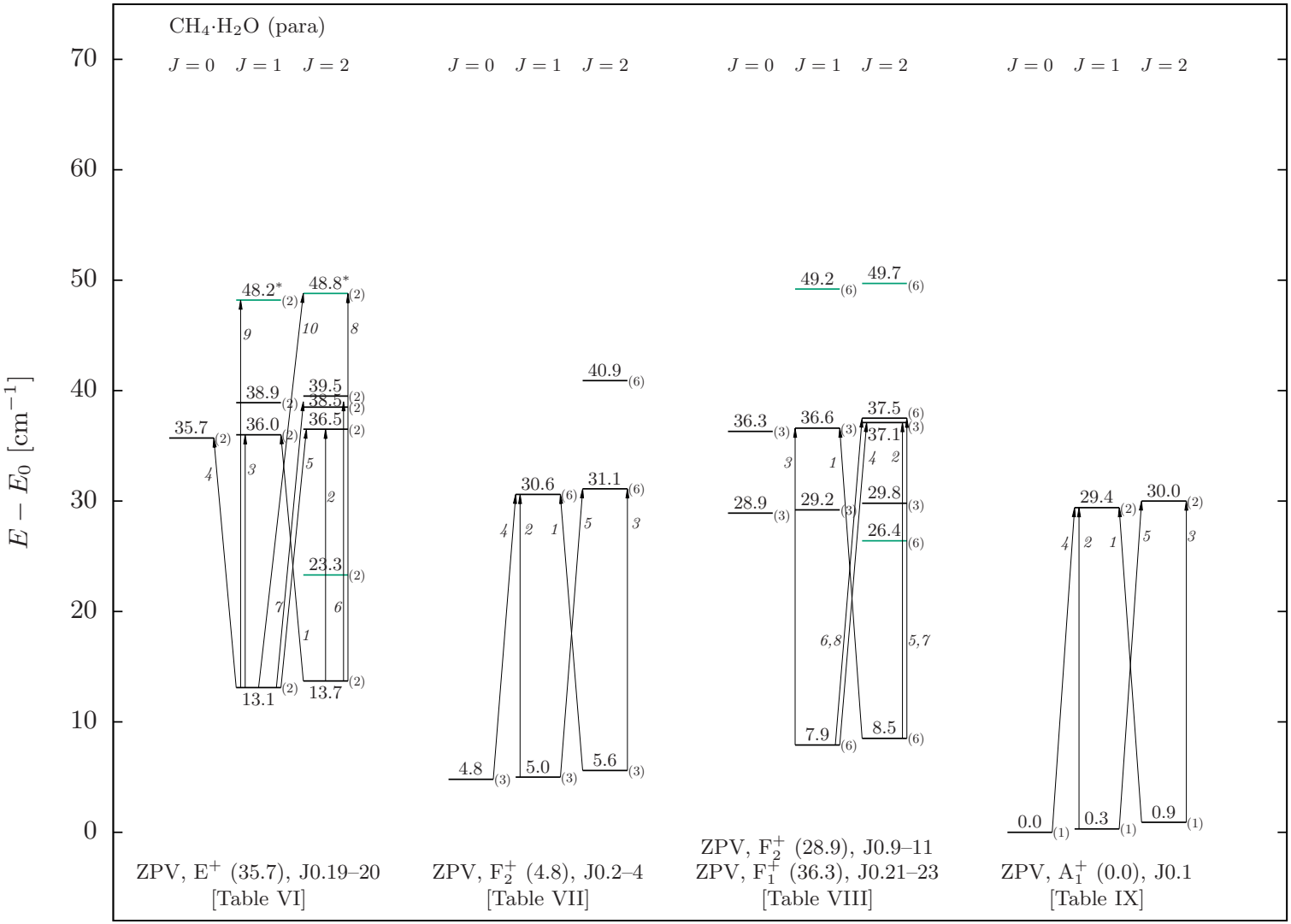

Deviation from experiment:
$(\Delta, \sigma) = (2, 0.01)$ cm^{-1}

[Exp.: JCP 100, 863 (1994)]

J. Sarka, A. G. Császár, S. C. Althorpe, D. J. Wales, and E. Mátyus, Phys. Chem. Chem. Phys. 18, 22816 (2016).

Outline of the talk

- Introduction
- Variational rovibrational computations
- Rovibrational results for $CH_4 \cdot H_2O$
- Deuterated isotopologues
- The coupled-rotors picture

Deuterated isotopologues of G_{48} symmetry

Vibrational states of $CX_4 \cdot Y_2O$ (X,Y = H,D)

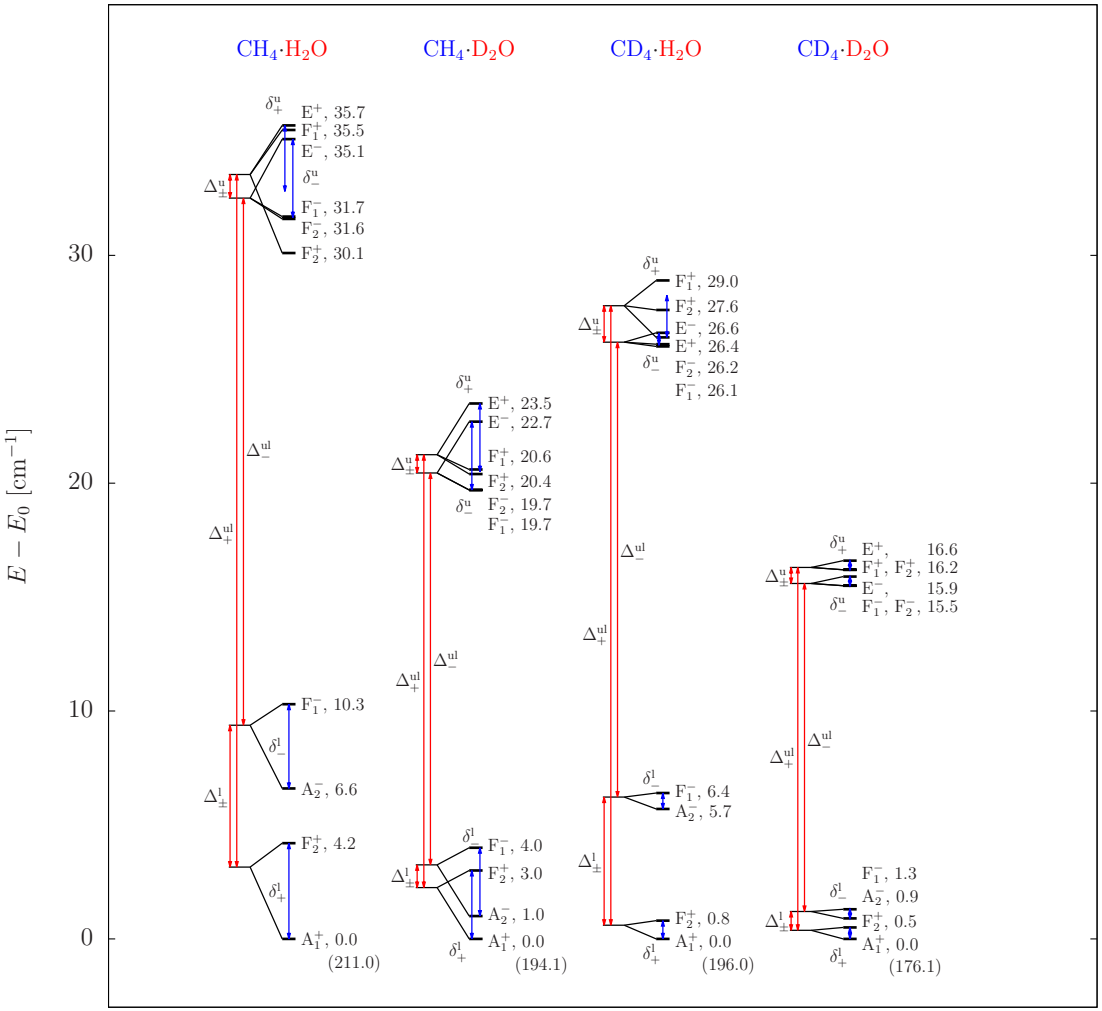

$CH_4 \cdot H_2O$, $CH_4 \cdot D_2O$,
$CD_4 \cdot H_2O$, $CD_4 \cdot D_2O$:

- similar vibrational splitting pattern
- characteristic upper-lower separation

J. Sarka, A. G. Császár, and E. Mátyus, PCCP 19, 15335 (2017).

Deuterated isotopologues of G_{48} symmetry

Rovibrational states of $CX_4 \cdot Y_2O$ (X,Y = H,D), Γ^+ symmetry

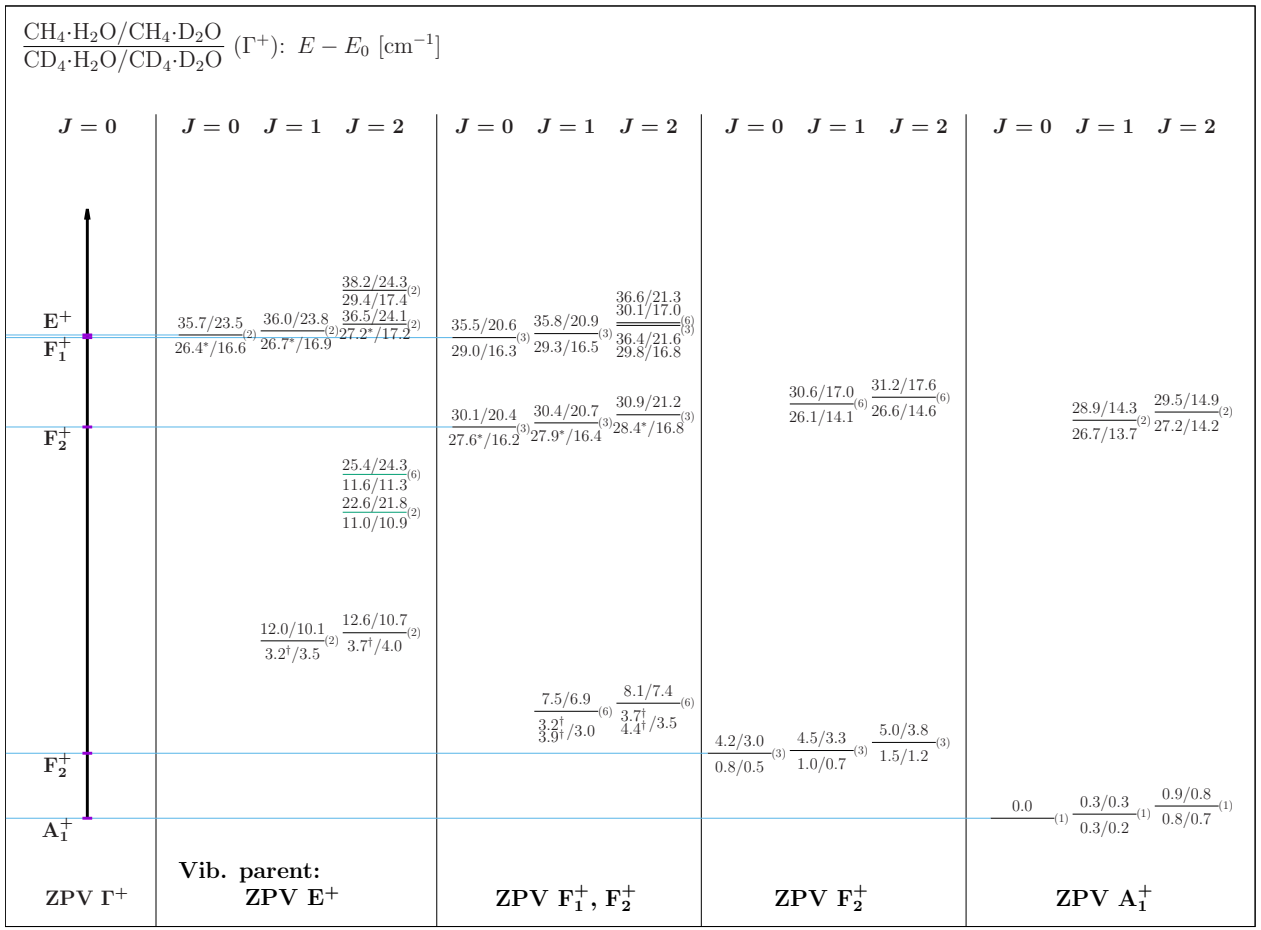

- the splitting values are different but the pattern is very similar for the isotopologues

Deuterated isotopologues of G_{48} symmetry

Rovibrational states of $CX_4 \cdot Y_2O$ (X,Y = H,D), Γ^- symmetry

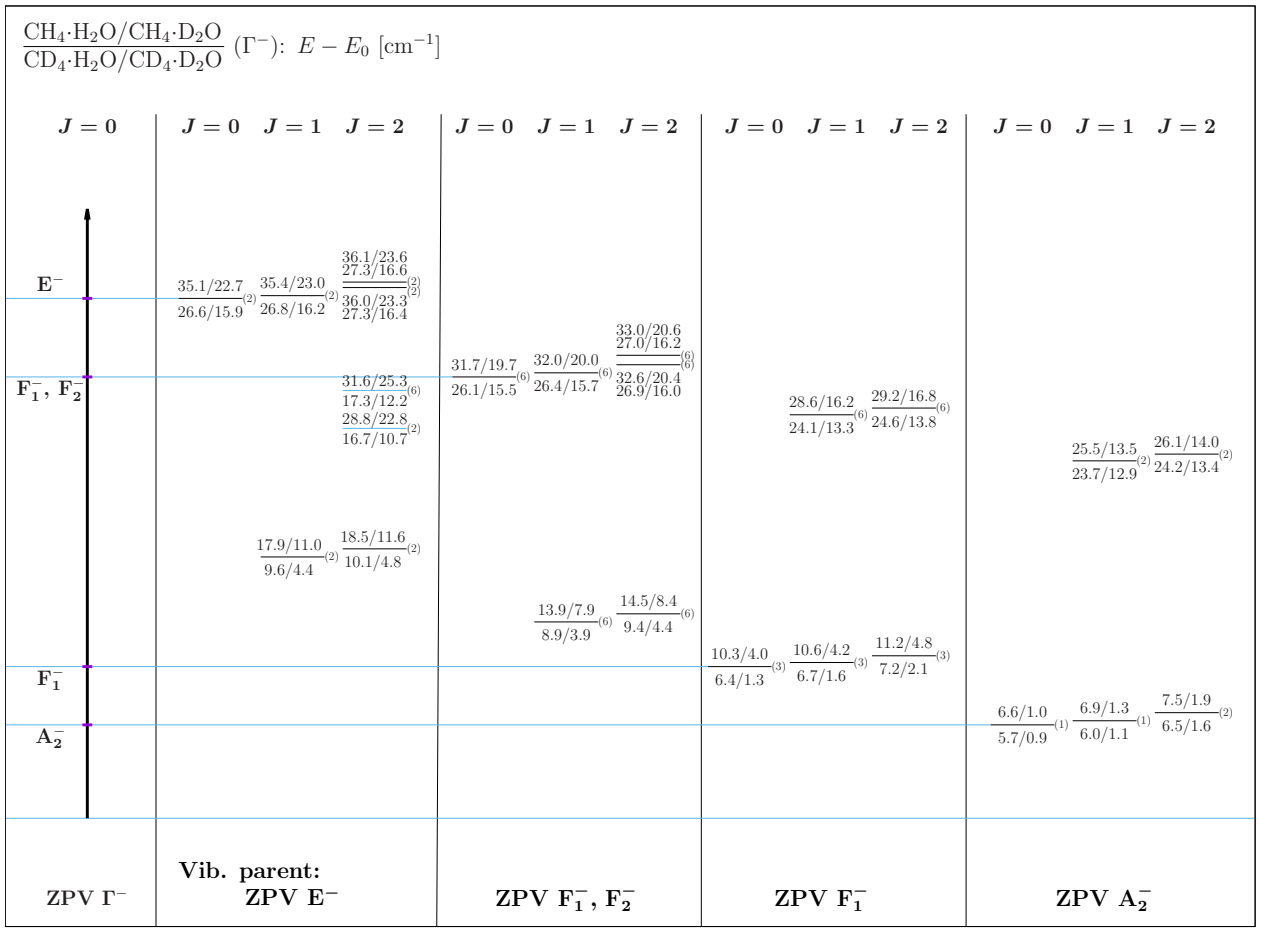

- the splitting values are different but the pattern is very similar for the isotopologues

Reversed rovibrational sequences

Regular

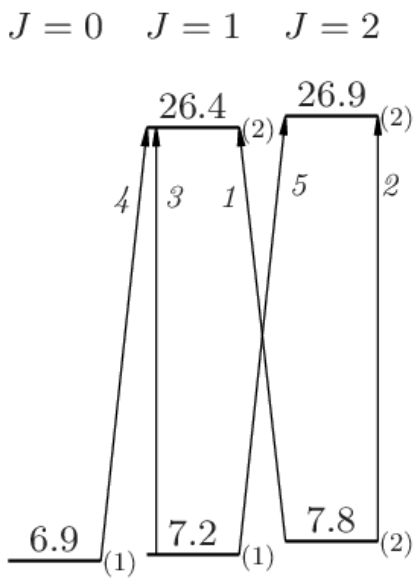

ZPV, A_2^- (6.9)

Reversed

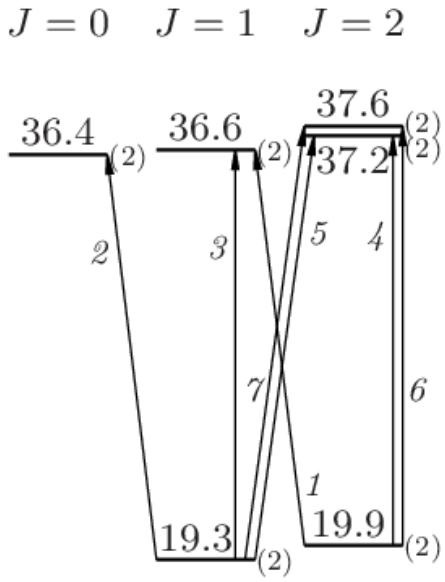

ZPV, E^- (36.4)

Reversed rovibrational sequences

- formally **"negative" rotational excitation energies** are present in certain vibrational bands (ZPV E^+, F_1^+, F_2^+, E^-, F_1^-, and F_2^-) in all $CX_4 \cdot Y_2O$ (X,Y = H,D) isotopologues
- also present in the **experimental data** reported for $CH_4 \cdot H_2O$ [JCP 100, 863 (1994)]

J. Sarka, A. G. Császár, and E. Mátyus, PCCP 19, 15335 (2017).

Outline of the talk

- Introduction
- Variational rovibrational computations
- Rovibrational results for $CH_4 \cdot H_2O$: theory vs. experiment
- Deuterated isotopologues
- The coupled-rotors picture

The coupled-rotors picture

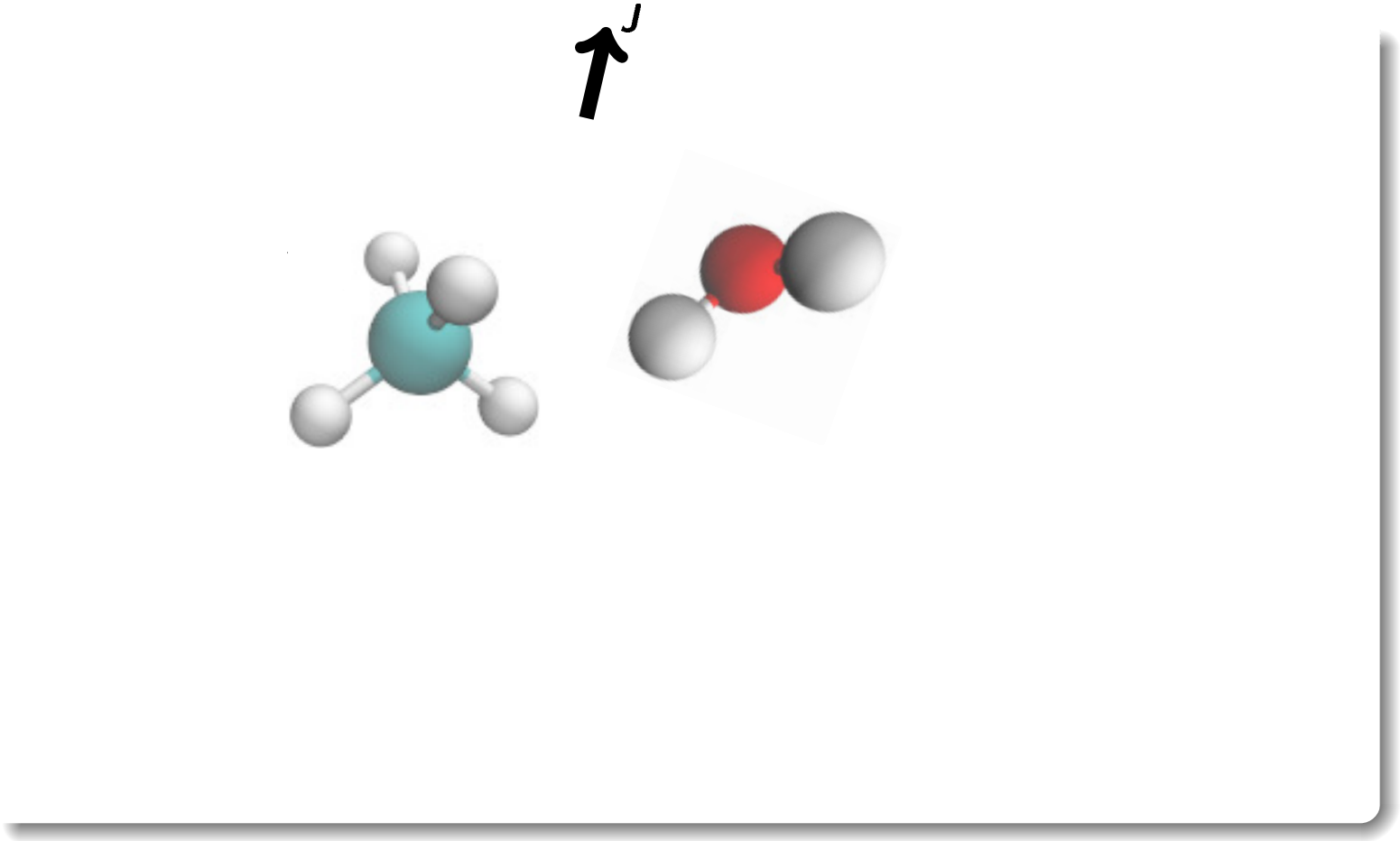

J. Sarka, A. G. Császár, and E. Mátyus, PCCP 19, 15335 (2017).

The coupled-rotors picture

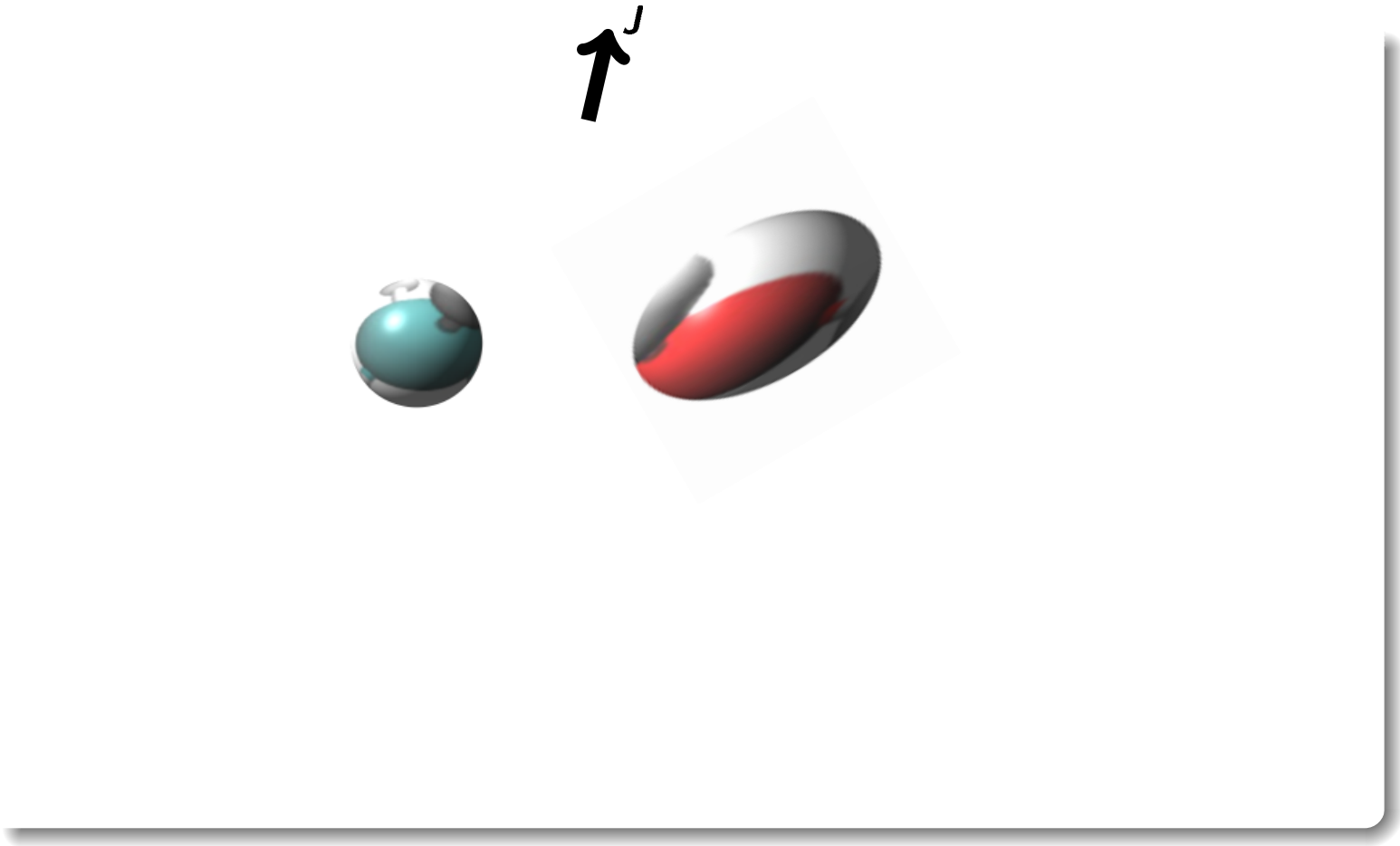

J. Sarka, A. G. Császár, and E. Mátyus, PCCP 19, 15335 (2017).

The coupled-rotors picture

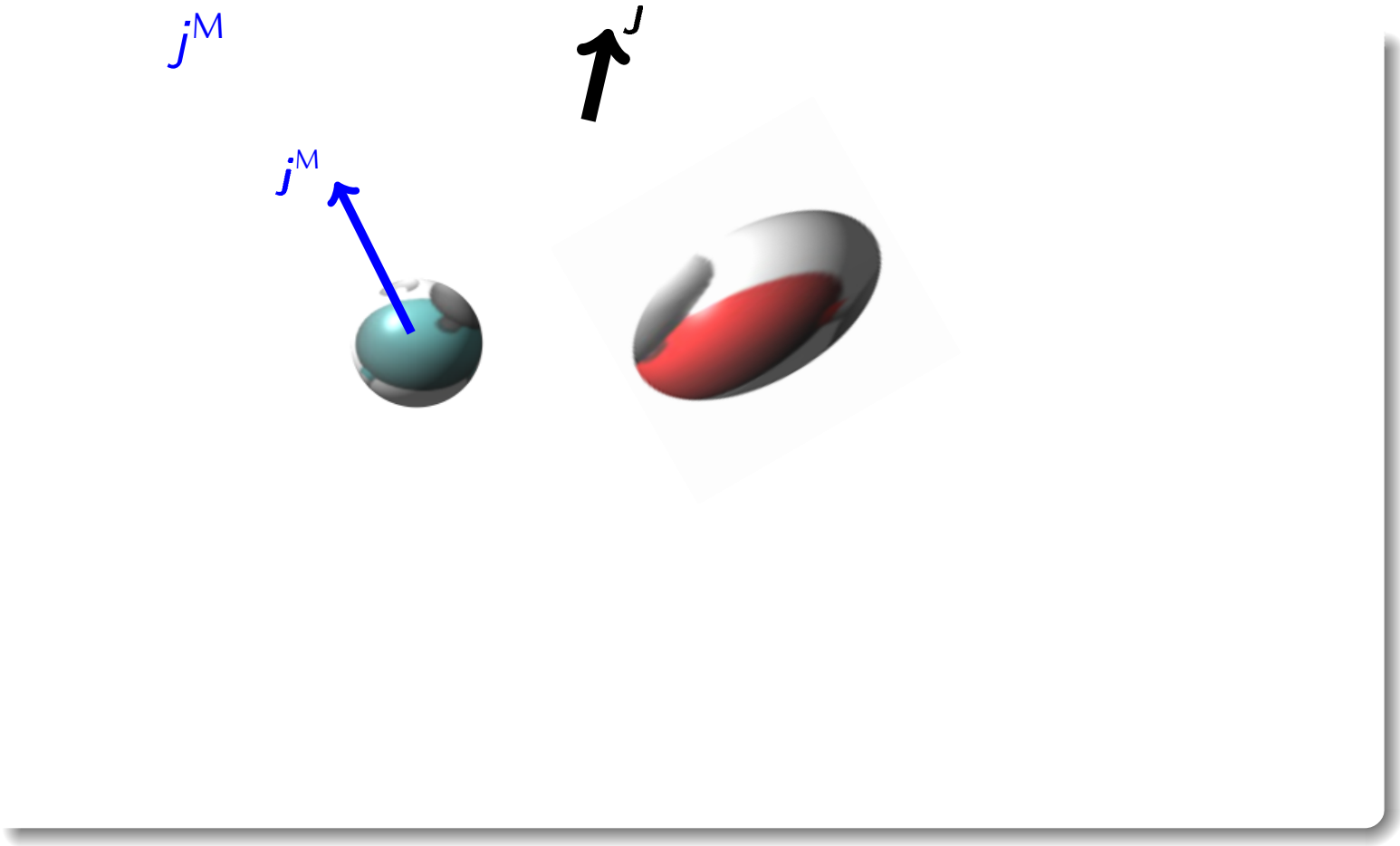

J. Sarka, A. G. Császár, and E. Mátyus, PCCP 19, 15335 (2017).

The coupled-rotors picture

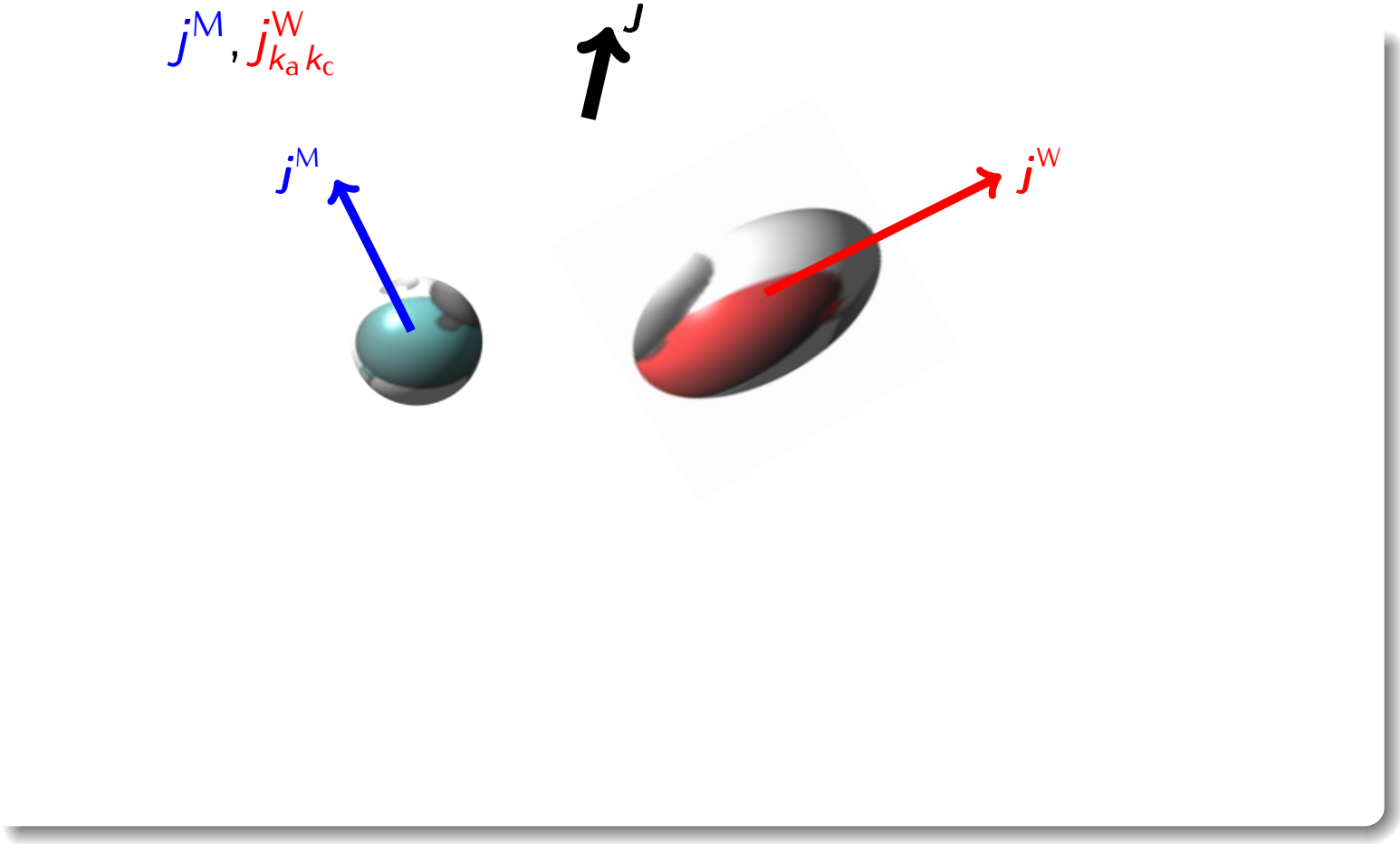

J. Sarka, A. G. Császár, and E. Mátyus, PCCP 19, 15335 (2017).

The coupled-rotors picture

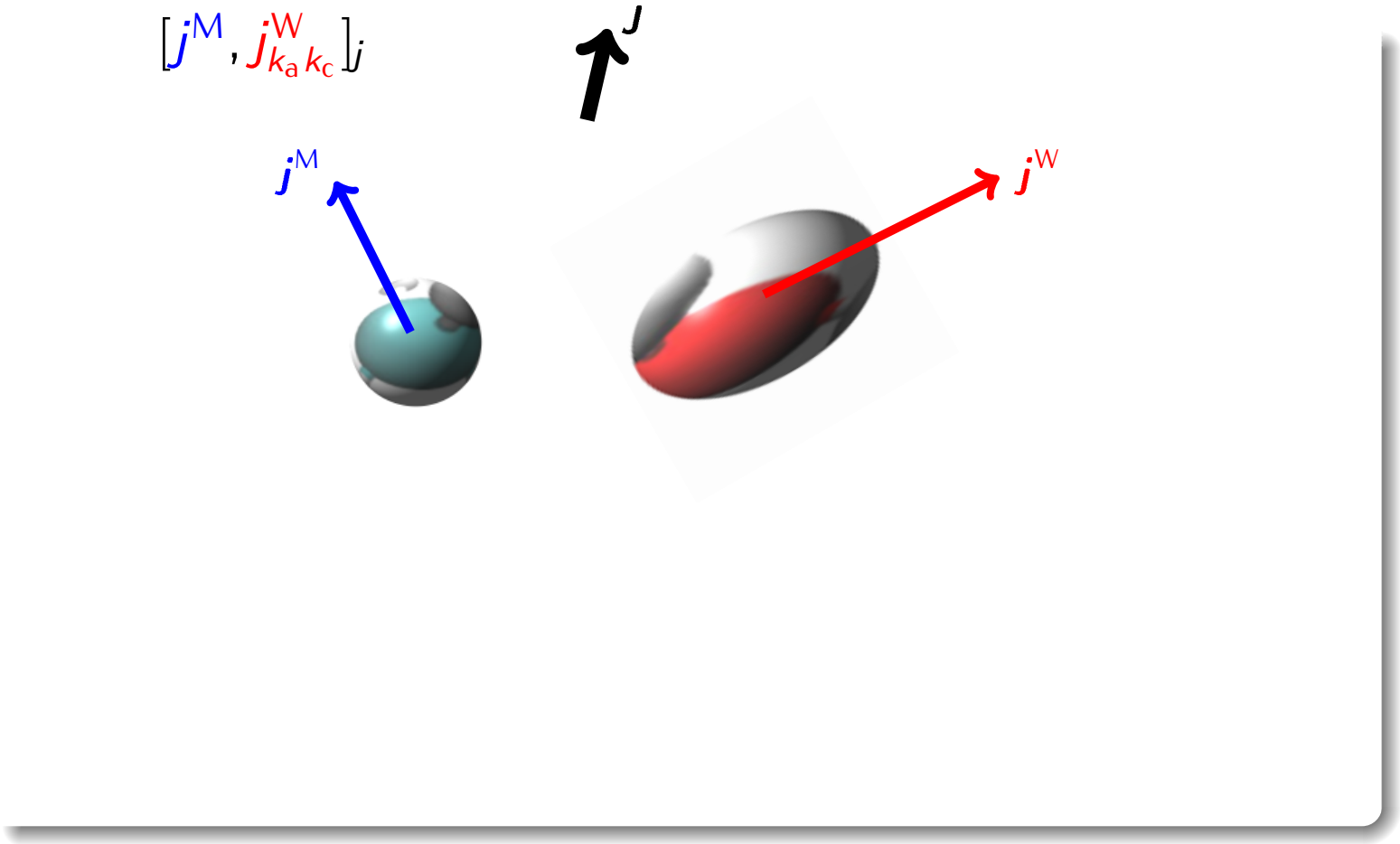

J. Sarka, A. G. Császár, and E. Mátyus, PCCP 19, 15335 (2017).

The coupled-rotors picture

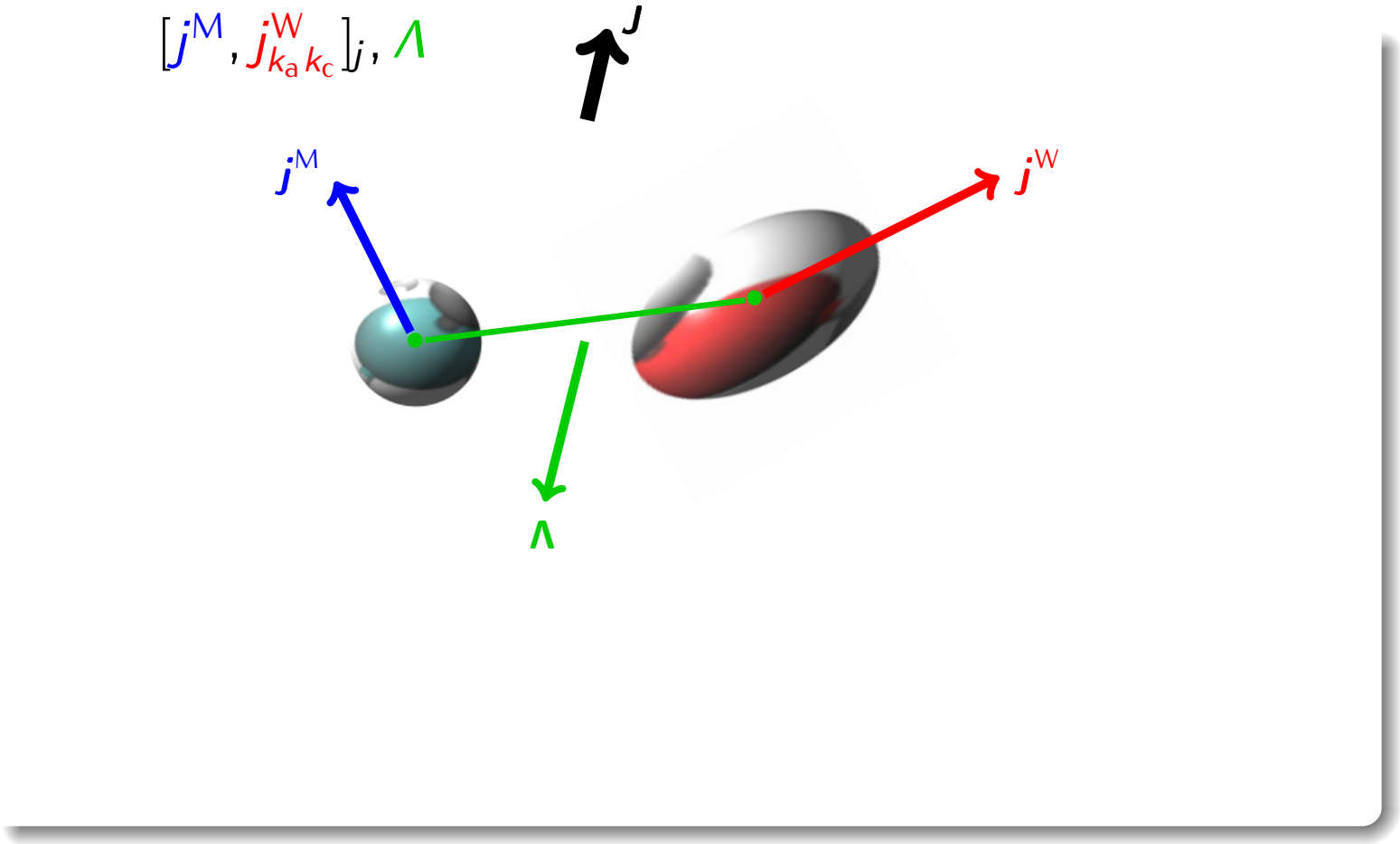

J. Sarka, A. G. Császár, and E. Mátyus, PCCP 19, 15335 (2017).

The coupled-rotors picture

$$[[j^{M}, j^{W}_{k_a k_c}]_j, \Lambda]_{JM}$$

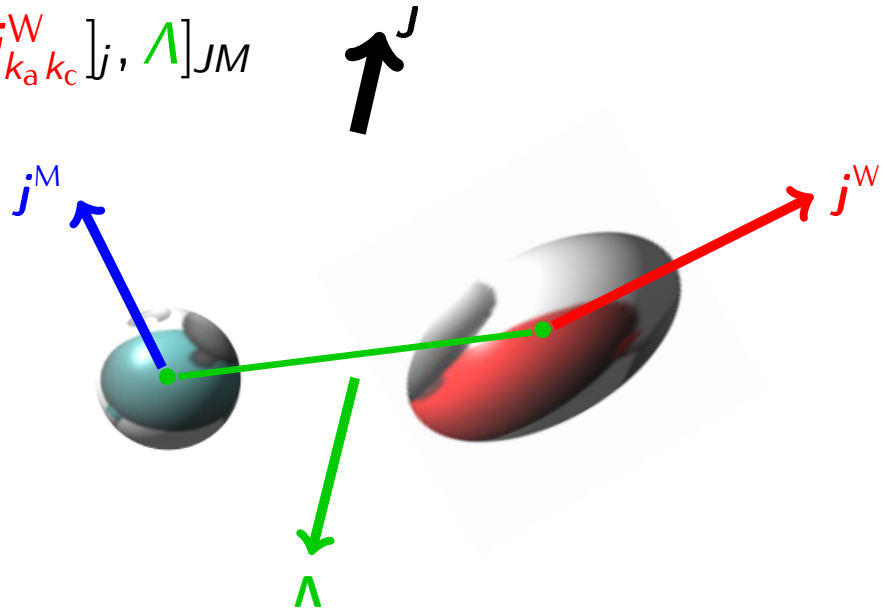

J. Sarka, A. G. Császár, and E. Mátyus, PCCP 19, 15335 (2017).

The coupled-rotors picture

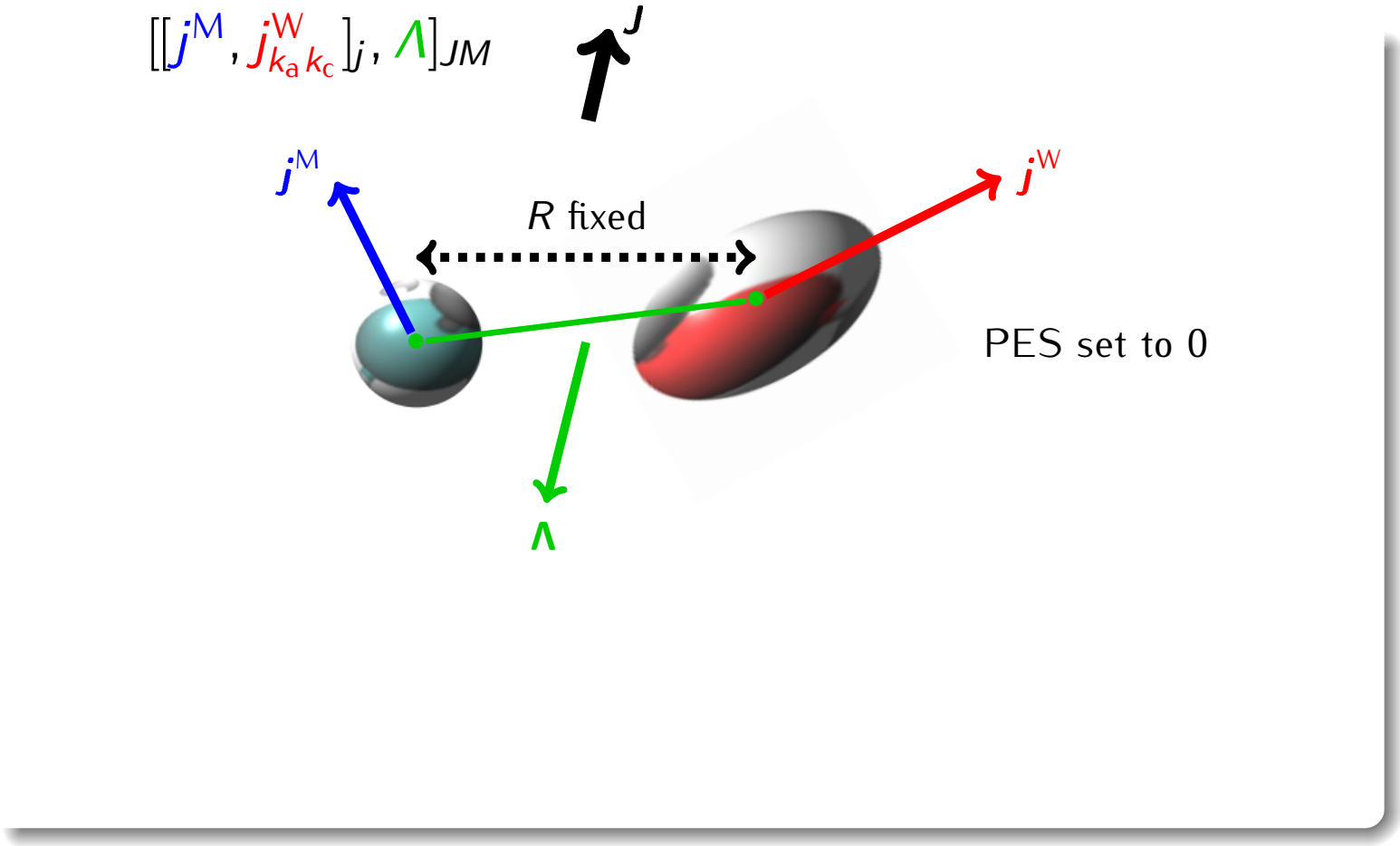

J. Sarka, A. G. Császár, and E. Mátyus, PCCP 19, 15335 (2017).

The coupled-rotors picture

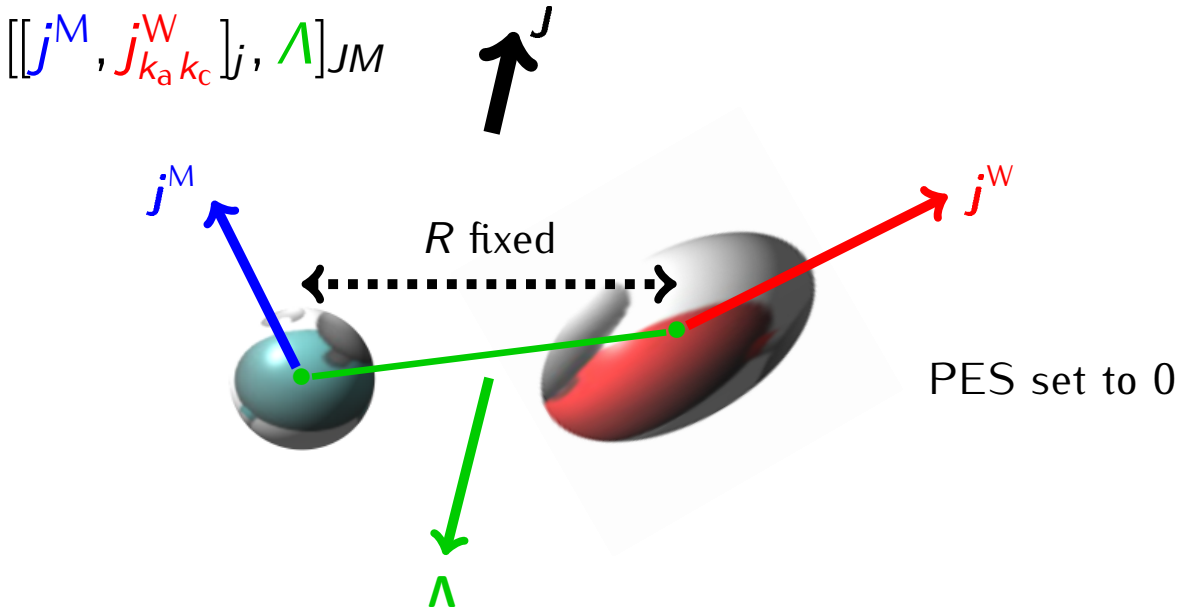

- solve this reduced-dimensional model (with $V = 0$) using GENIUSH to obtain the coupled-rotors states in the same angular grid representation as the full problem

J. Sarka, A. G. Császár, and E. Mátyus, PCCP 19, 15335 (2017).

Symmetry of the coupled-rotors functions

Γ	E	(123)	(14)(23)	[(1423)(ab)]*	[(23)(ab)]*	(ab)	(123)(ab)	(14)(23)(ab)	[(1423)]*	[(23)]*	Irreps
	1	8	3	6	6	1	8	3	6	6	
$[[0,0_{00}]_0,0]_0$	1	1	1	1	1	1	1	1	1	1	A_1^+
$[[0,1_{11}]_1,1]_0$	1	1	1	1	1	1	1	1	1	1	A_1^+
$[[1,0_{00}]_1,1]_0$	3	0	−1	−1	1	3	0	−1	−1	1	F_2^+
$[[1,1_{11}]_0,0]_0$	3	0	−1	−1	1	3	0	−1	−1	1	F_2^+
$[[1,1_{11}]_1,1]_0$	3	0	−1	1	−1	3	0	−1	1	−1	F_1^+
$[[1,1_{11}]_2,2]_0$	3	0	−1	−1	1	3	0	−1	−1	1	F_2^+
$[[2,0_{00}]_2,2]_0$	5	−1	1	−1	1	5	−1	1	−1	1	$E^+ \oplus F_2^+$
$[[2,1_{11}]_1,1]_0$	5	−1	1	−1	1	5	−1	1	−1	1	$E^+ \oplus F_2^+$
$[[2,1_{11}]_2,2]_0$	5	−1	1	1	−1	5	−1	1	1	−1	$E^+ \oplus F_1^+$
$[[2,1_{11}]_3,3]_0$	5	−1	1	−1	1	5	−1	1	−1	1	$E^+ \oplus F_2^+$
$[[0,1_{01}]_1,1]_0$	1	1	1	−1	−1	−1	−1	−1	1	1	A_2^-
$[[0,1_{10}]_1,1]_0$	1	1	1	1	1	−1	−1	−1	−1	−1	A_1^-
$[[1,1_{01}]_0,0]_0$	3	0	−1	1	−1	−3	0	1	−1	1	F_1^-
$[[1,1_{01}]_1,1]_0$	3	0	−1	−1	1	−3	0	1	1	−1	F_2^-
$[[1,1_{01}]_2,2]_0$	3	0	−1	1	−1	−3	0	1	−1	1	F_1^-
$[[1,1_{10}]_0,0]_0$	3	0	−1	−1	1	−3	0	1	1	−1	F_2^-
$[[1,1_{10}]_1,1]_0$	3	0	−1	1	−1	−3	0	1	−1	1	F_1^-
$[[1,1_{10}]_2,2]_0$	3	0	−1	−1	1	−3	0	1	1	−1	F_2^-
$[[2,1_{01}]_1,1]_0$	5	−1	1	1	−1	−5	1	−1	−1	1	$E^- \oplus F_1^-$
$[[2,1_{01}]_2,2]_0$	5	−1	1	−1	1	−5	1	−1	1	−1	$E^- \oplus F_2^-$
$[[2,1_{01}]_3,3]_0$	5	−1	1	1	−1	−5	1	−1	−1	1	$E^- \oplus F_1^-$
$[[2,1_{10}]_1,1]_0$	5	−1	1	−1	1	−5	1	−1	1	−1	$E^- \oplus F_2^-$
$[[2,1_{10}]_2,2]_0$	5	−1	1	1	−1	−5	1	−1	−1	1	$E^- \oplus F_1^-$
$[[2,1_{10}]_3,3]_0$	5	−1	1	−1	1	−5	1	−1	1	−1	$E^- \oplus F_2^-$

J. Sarka, A. G. Császár, and E. Mátyus, PCCP 19, 15335 (2017).

Coupled-rotors decomposition

Overlap of the full intermolecular wave function and the coupled rotors functions

$$\mathrm{CRD}^{(J)}_{nm} = \sum_{r=1}^{N_R} \left| \sum_{k=-J}^{J} \sum_{o=1}^{N_\Omega} \tilde{\Psi}^{(J)}_{n,k}(\rho_r, \boldsymbol{\omega}_o) \cdot \tilde{\varphi}^{(J)}_{m,k}(\boldsymbol{\omega}_o) \right|^2$$

- sum of columns $= 1$
- sum of rows ≥ 1

$\Rightarrow$ j^{M}, $j^{\mathrm{W}}_{k_a k_c}$, and Λ labels

$\Rightarrow$ automated symmetry assignment (irreps of the G_{48} group)

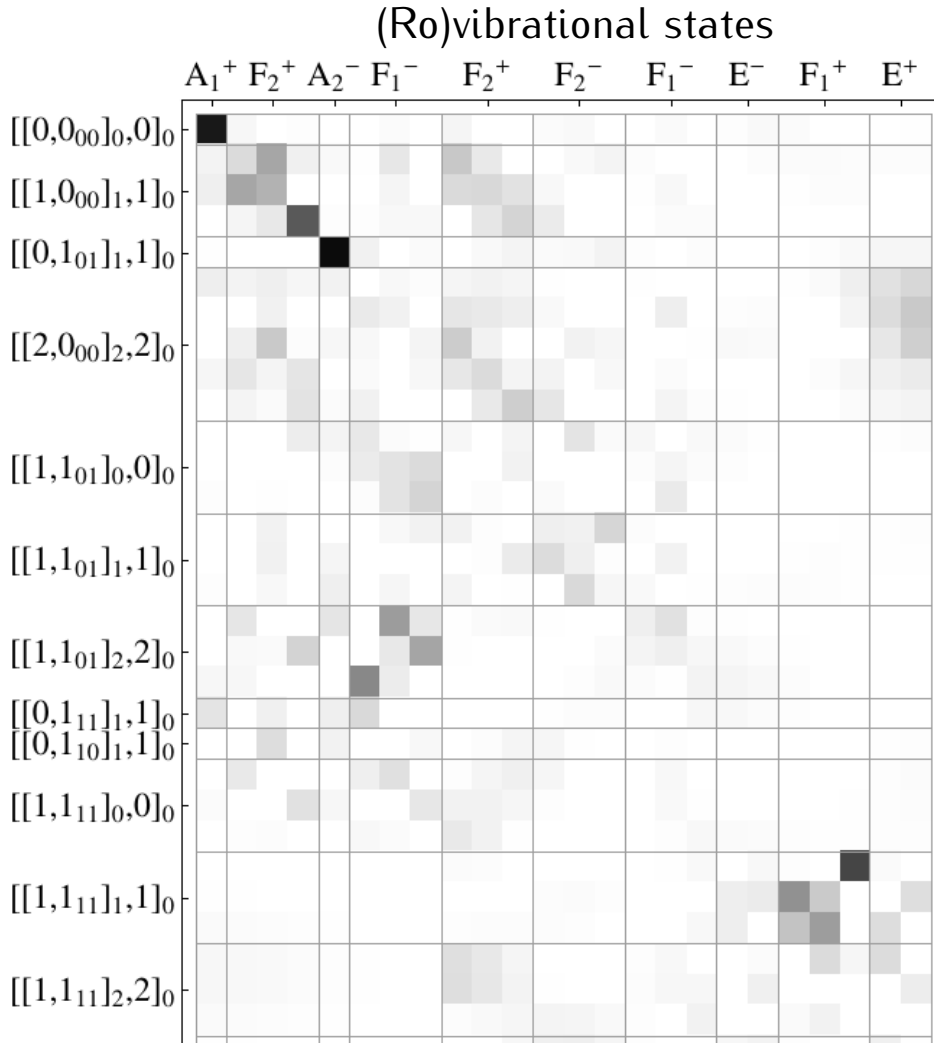

J. Sarka, A. G. Császár, and E. Mátyus, PCCP 19, 15335 (2017).

Rovibrational states of $CX_4 \cdot Y_2O$ (X,Y = H,D), Γ^+ symmetry

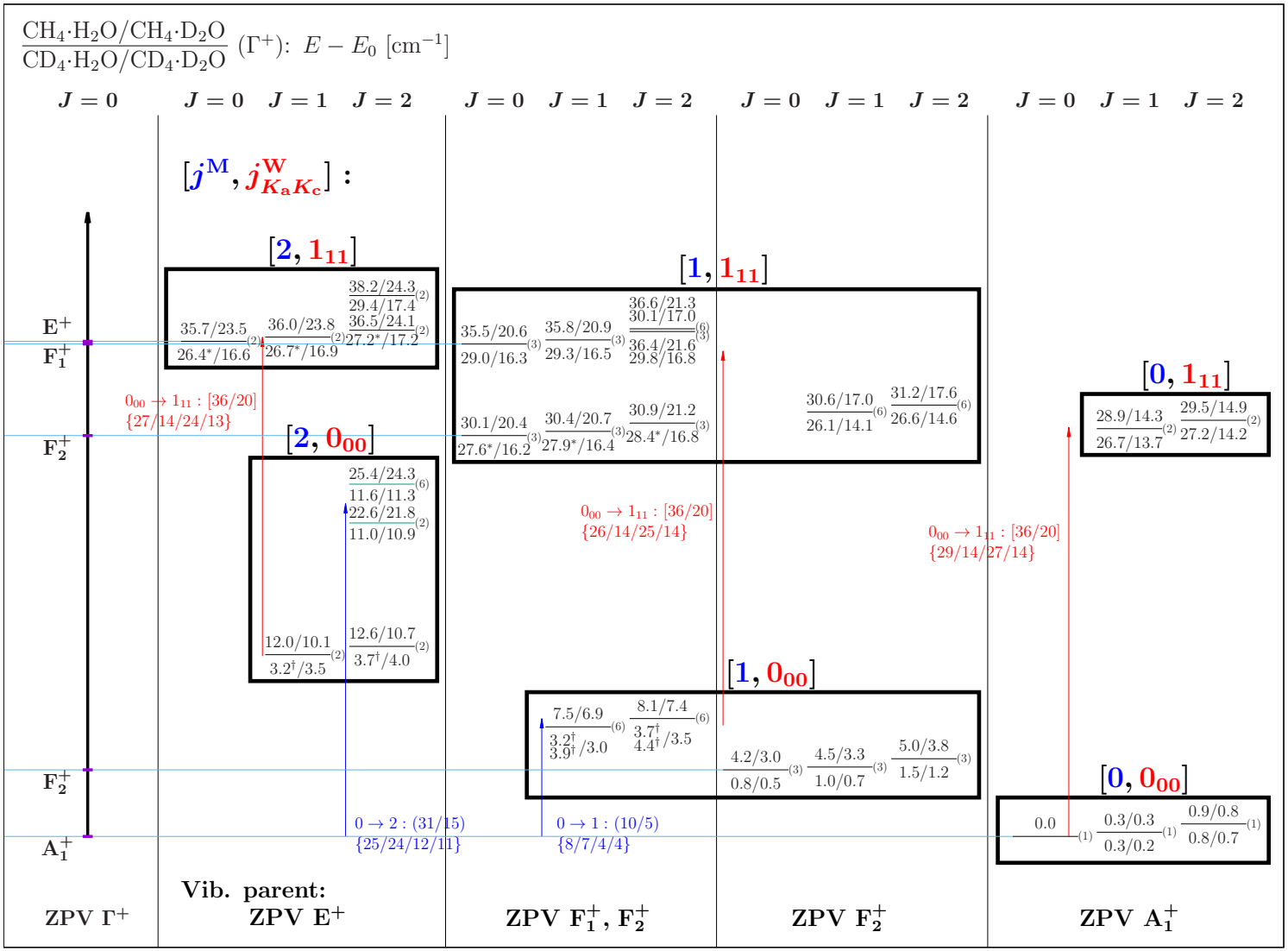

J. Sarka, A. G. Császár, and E. Mátyus, PCCP 19, 15335 (2017).

Rovibrational states of $CX_4 \cdot Y_2O$ (X,Y = H,D), Γ^- symmetry

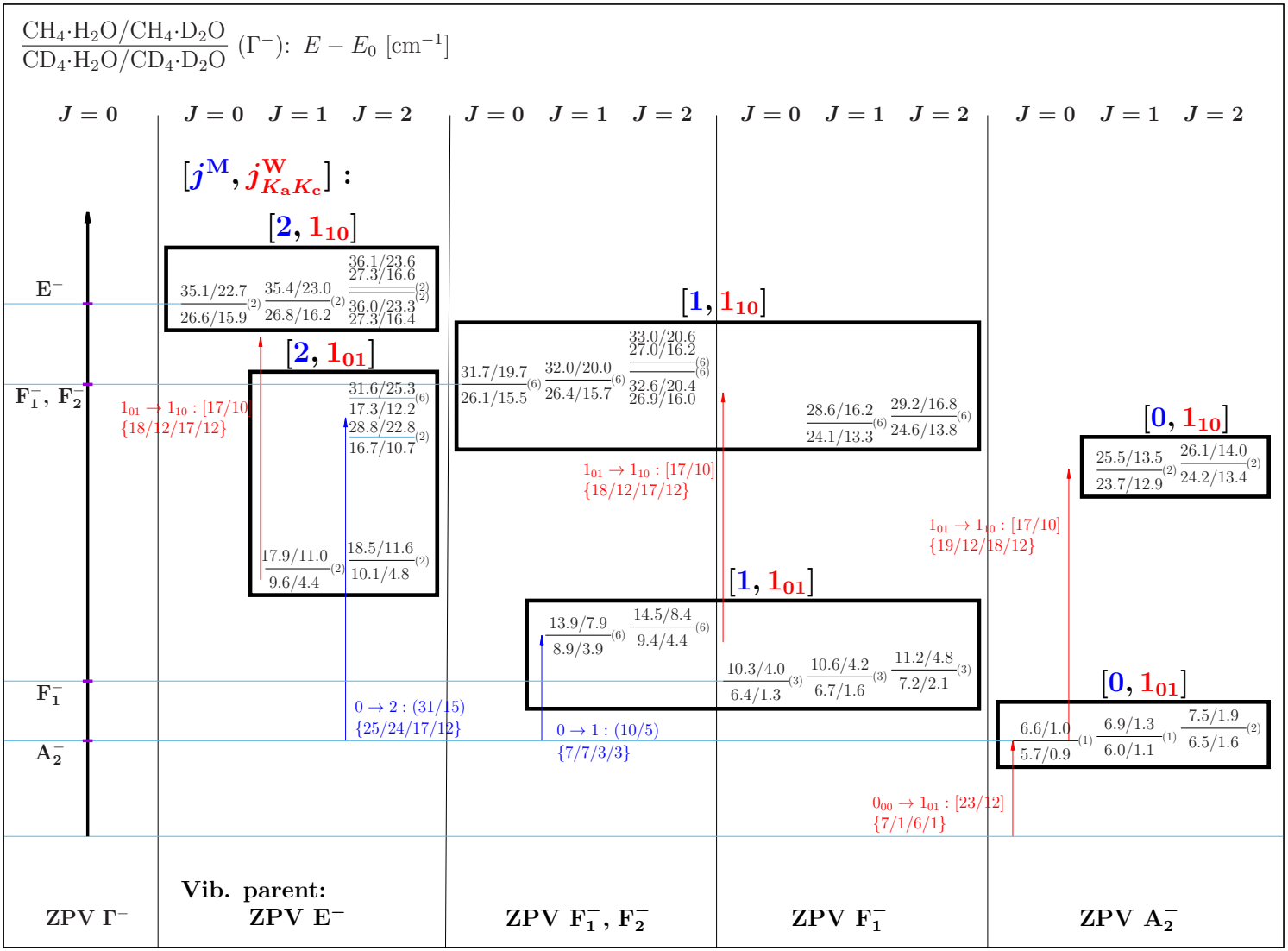

J. Sarka, A. G. Császár, and E. Mátyus, PCCP 19, 15335 (2017).

Summary

All experimentally reported transitions

- have been identified in the computations
- take place within the **rovibrational ZPV manifold of the global minimum**.

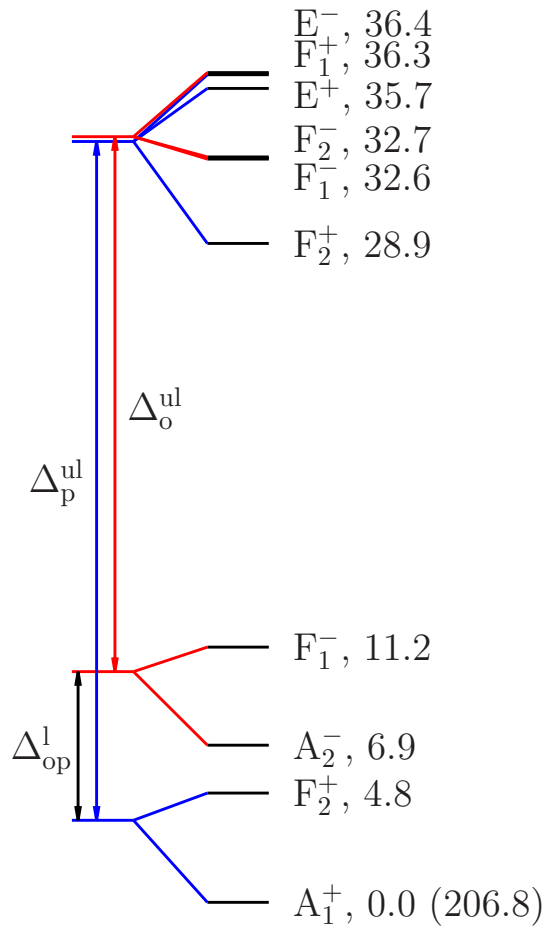

Summary

All experimentally reported transitions

- have been identified in the computations
- take place within the **rovibrational ZPV manifold of the global minimum**.

Theoretical predictions of

- transitions to states assigned to the **secondary minimum** might be confirmed experimentally in the future (exchanged roles of the hydrogen donor and acceptor).

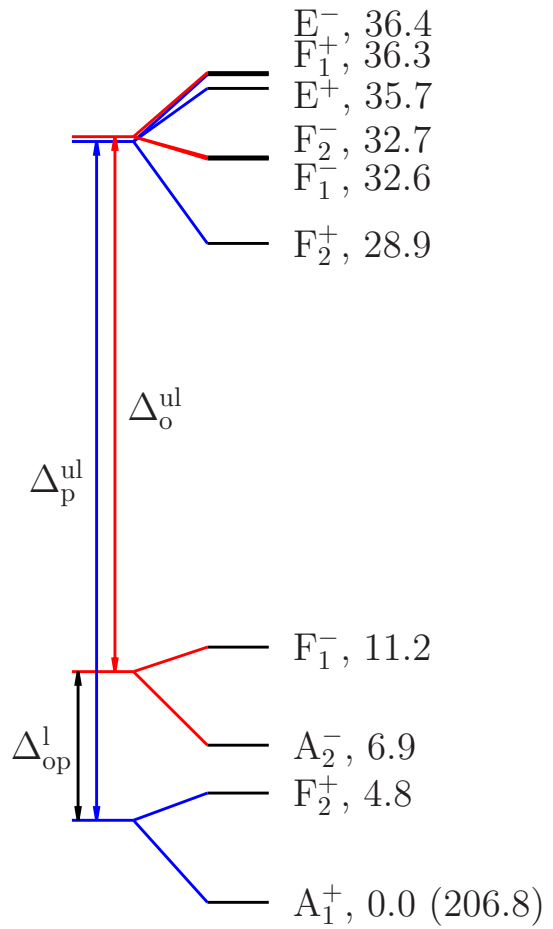

Summary

All experimentally reported transitions

- have been identified in the computations
- take place within the **rovibrational ZPV manifold of the global minimum**.

Theoretical predictions of

- transitions to states assigned to the **secondary minimum** might be confirmed experimentally in the future (exchanged roles of the hydrogen donor and acceptor).

Similar ZPV splitting pattern

- were found for all $CX_4 \cdot Y_2O$ (X,Y=H,D) **isotopologues**.

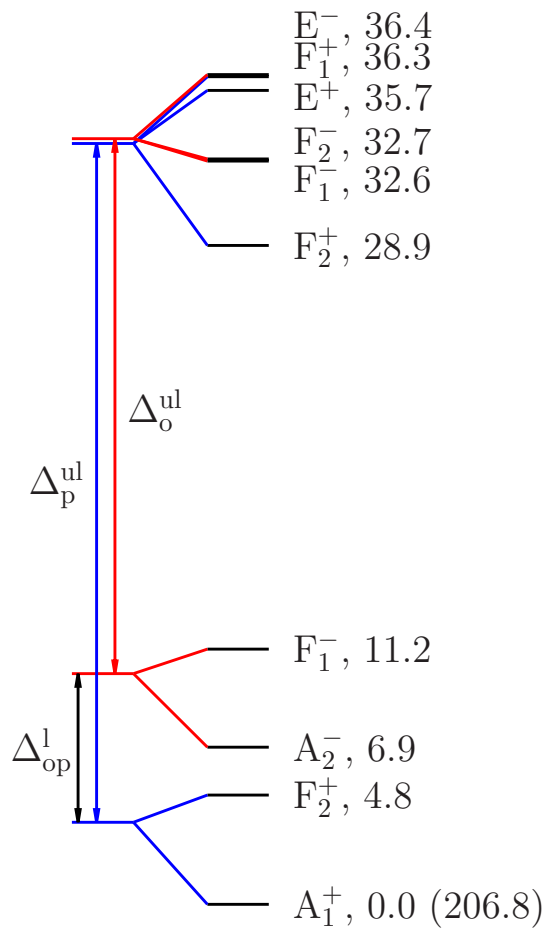

Summary

All experimentally reported transitions

- have been identified in the computations
- take place within the **rovibrational ZPV manifold of the global minimum**.

Theoretical predictions of

- transitions to states assigned to the **secondary minimum** might be confirmed experimentally in the future (exchanged roles of the hydrogen donor and acceptor).

Similar ZPV splitting pattern

- were found for all $CX_4 \cdot Y_2O$ (X,Y=H,D) **isotopologues**.

Coupled-rotors picture

- helps to understand the **negative-energy rotational excitations**.

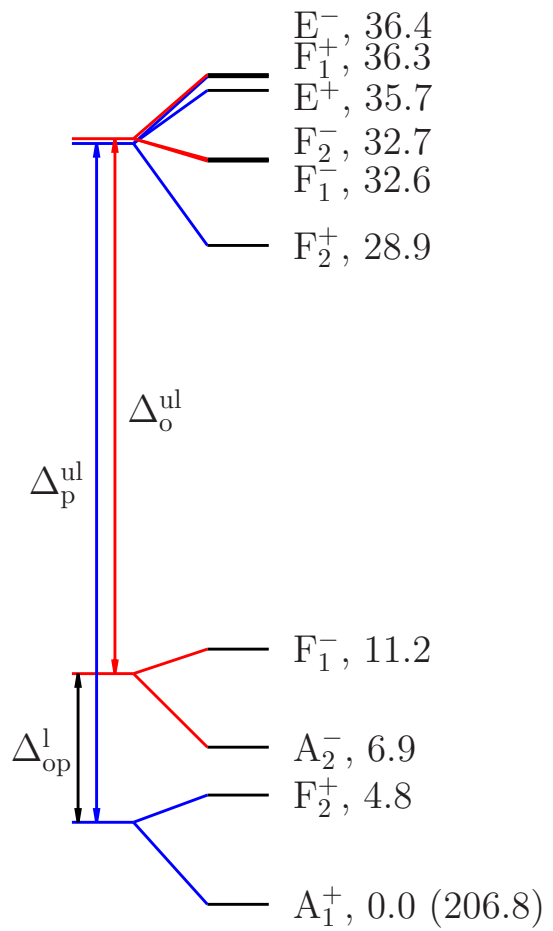

Acknowledgement

- **Prof. Stuart Althorpe** (Cambridge)
- **Prof. David Wales** (Cambridge)

- **computing infrastructure** of the Laboratory of Molecular Structure and Dynamics (ELTE) & Complex Chemical Systems Research Group (MTA-ELTE)

- **ÚNKP**-16-3 New National Excellence Program of the Ministry of Human Capacities of Hungary
- **NKFIH** (grant no. K119658).
- the COST Action CM1405 entitled **MOLIM**: Molecules in Motion
- a **PROMYS Grant** (no. IZ11Z0_166525) of the Swiss National Science Foundation

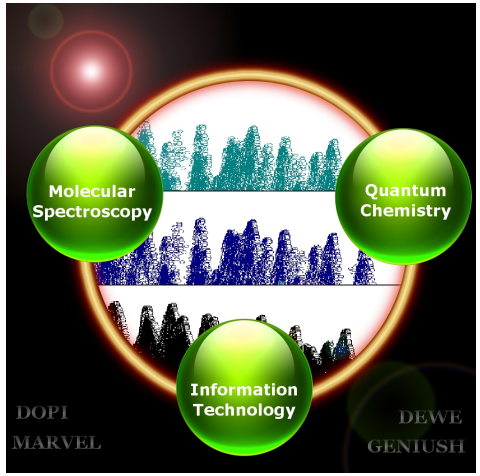

Emberi Erőforrások Minisztériuma